Numerical simulation of primary breakup of nonturbulent liquid jets in high-viscous gaseous crossflows

Mohammad Hashemi*[1], Mehdi Jadidi[1], Ali Dolatabadi[1]
[1]Department of Mechanical, Industrial and Aerospace Engineering, Concordia University, Montreal, QC, Canada H3G 2W1
Corresponding author: mo_ashem@encs.concordia.ca

Abstract
Atomization of liquid jets in subsonic gaseous crossflows is of great importance in thermal spray coating process. In this process, suspensions and solution precursors are injected into high-viscous plasma crossflows where the gas-flow Reynolds and Weber numbers are around 50 and 200, respectively. The coatings' quality strongly depends on the breakup of liquid jets in plasma crossflows. In the absence of comprehensive atomization measurements, robust numerical simulations have suggested a detailed picture of atomization process in recent years. In this work, a numerical model is used to investigate the impact of gas viscosity on breakup mechanisms. The conservation of mass and momentum, and capturing the interface are solved by a computational fluid dynamics (CFD) code, called Basilisk. The incompressible variable-density Navier–Stokes (NS) equations are solved by using finite volume schemes. The gas-liquid interface is tracked by a geometric volume-of-fluid (VOF) approach. A parametric study is performed on atomization process in a wide range of gas-flow Reynolds numbers (Reg=39−39000). The jet trajectory, breakup location and instability waves generated along the jet column are investigated. Ultimately, the effect of gas viscosity on jet deformation and breakup physics are described.

Keywords
Atomization; Crossflow; Gas-flow Reynolds numbers; Thermal spray; Numerical simulation

Introduction
The dispersion of liquid bulk into small droplets in a secondary fluid phase, which is known as atomization, is vastly observed in many industrial and environmental processes. This mechanism has several applications in combustion, meteorology and medicine. The atomization process has three main steps: the ejection of liquid from atomizer, the primary and secondary breakup mechanisms.
Some theoretical analyses found the connection between the jet breakup and the unstable waves evolving on the liquid-gas interface. The first two breakup regimes, which are Rayleigh and first wind-induced breakup regime respectively, were well predicted by temporal stability analysis in the work of Sterling and Sleicher [1]. In this study, it was assumed that the interface of a circular jet is perturbed by an axisymmetric wave with a Fourier component of the form

$$\eta = \eta_0 \exp(\omega t + ikx), \quad (1)$$

Where $\eta = \eta(x,t)$ is the displacement of the liquid surface. η_0 is the initial amplitude of the disturbance. The fluid is located at the nozzle exit, $x = 0$, when $t = 0$. k is the wave number of the disturbance and ω is the complex frequency which its real component indicates the growth rate of surface displacement. Based on the linear stability analysis of jet interface, a dispersion equation explains the relation of the complex frequency of an initial perturbation to its wave number. The shortcomings and limitations of theoretical analysis made the importance of experimental data significant. In many experimental studies, the achievements were summarized as correlations between jet characteristics (such as breakup length, average droplet size and cone angle) and experiment setups (for instance, material properties, atomizer design and injection pressure). The first experimental investigation is related to the first half of nineteenth century. Cylindrical jets are generated by forcing liquid through a cylindrical tube. Based on the outlet velocity of the tube, the atomization regimes were classified. Therefore, jet breakup point can be plotted versus the average velocity of jet which can be calculated by dividing the flow rate by the outlet cross-section area of nozzle. This plot is known as jet stability curve. Many attempts [2–4] were done on gaining a more accurate jet stability curve.
Lin and Reitz [5] reviewed the different criteria applied for the jet breakup regimes existed in the literature. These summarized classifications are mainly based on non-dimensional numbers.

Comprehensive analytical study is not possible yet to consider the impacts of all forces involved in atomization, since no general exact solution was found to Navier-Stokes equations. On the other side, although the measurement devices have been improved, such as high speed cameras, the results do not provide sufficient details. So, the numerical solution to the complete form of Navier-Stokes equations is highly desirable to consider shear stress, inertia and surface tension forces, all together.

For the most of fluids, the length scales of tens of micrometer is still sufficient to apply continuum methods. In the continuum methods, Navier-Stokes equations satisfiy the physics. Also, an equation is solved to track the gas-liquid interface. The strategies were developed to solve the equation for interface evolution can grouped to five main methods: volume-of-fluid (VOF) method, level set, front-tracking, phase-field and moving mesh. In VOF, a scalar variable called color function, f, is defined where $f = 1$ and $f = 0$ represent the reference phase and the second phase respectively. So, everywhere else with $0 < f < 1.0$ is interface. Different concepts were defined to reconstruct the interface. In the earliest work on VOF methods, Noh and Woodward [6] used a simple line interface calculation (SLIC) and Hirt and Nichols [7] applied a stair-stepped interface representation. A more accurate reconstruction of interface is based on a method so-called piecewise linear interface calculation (PLIC) which approximate the interface in each cell by a line and plane in 2D and 3D, in respect. The normal of the plane (or line in 2D) is calculated based on the gradient of color function in the neighborhood of each cell. An early PLIC algorithm was suggested by Youngs [8]. A new generation of VOF was introduced by Ahn and Shashkov [9] which is called the moment-of-fluid. In this method, the material volume and the centroid of the reference phase are advected and the interface is reconstructed based on the updated centroid in each interface cell.

Level set (LS) method [10] suggests a smooth scalar function of position, $\varphi(\vec{x})$, as a signed distance from interface. So, the place of interface should be $\varphi(\vec{x}) = 0$. Sussman et al. [11] applied this method to two-phase flows. Handling complex geometry is the most important capability of LS method. Front-tracking (FT) method [12,13] proposed the idea of defining the interface as an explicit boundary by a discrete data structure which is updated in time loop to capture the movement of interface. Unverdi and Tryggvason [14] applied this approach in the simulation of bubble motion in a secondary fluid.

Various numerical models were suggested for incompressible multiphase systems which integrate CFD techniques with the mentioned interface tracking approaches. In the proposed models, the incompressible forms of Navier-Stokes equations for a mixture of two immiscible substances were solved. Xiao et al. [15] applied a large eddy simulation (LES) algorithm for the atomization of incompressible liquid jet in supersonic gas flow. The interface acts as a boundary between two phases for both compressible and incompressible solvers used in this study. Li et al. [16] investigated the impact of high liquid viscosity on jet atomization in crossflow. They solved the incompressible two-phase flow of liquid and gas by a single-fluid formulation. In this work, a computational code [17,18], based on a coupled level set and volume-of-fluid method (CLSVOF), was utilized which is called HiMIST.

Liquid jet in gaseous crossflow has tremendous applications such as fuel injection in gas turbines [19] and suspension injection in thermal spray to manufacture nanostructured coatings [20]. In general, liquid jets in subsonic gas crossflows are usually classified based on the turbulence of liquid jet and uniform/nonuniform inlet profile of crossflow. Mazallon et al. [21] studied the injection of nonturbulent liquid jet into a uniform crossflow. They categorized breakup regimes into four groups, namely column, bag, multimode, and shear breakup. Lee et al. [22] proposed that bag and multimode breakup regimes are not observed for turbulent jets in uniform crossflow at low weber numbers.

In this paper, a numerical model is used to investigate the impact of gas viscosity on atomization mechanisms. The conservation of mass and momentum, and capturing the interface are solved by a numerical multiphase flow solver, known as Basilisk [23]. The incompressible variable-density Navier–Stokes (NS) equations are solved by using finite volume schemes. The gas-liquid interface is tracked by a geometric VOF approach. A parametric study is performed on atomization process in a wide range of gas-flow Reynolds numbers (Reg=39−39000). The mass flow rate, size and velocity of droplets generated along the jet column are investigated. Ultimately, the effect of gas viscosity on jet deformation and breakup physics are analyzed.

Methodology

The incompressible variable-density form of Navier–Stokes equations are solved for a mixture of two immiscible substances at low Mach number. The two-phase flow of liquid and gas is presented by a single fluid formulation. The continuity and momentum equations are

$$\nabla . \boldsymbol{u} = 0, \tag{2}$$

$$\rho \frac{\partial \boldsymbol{u}}{\partial t} + \rho \boldsymbol{u} . \nabla \boldsymbol{u} = -\nabla p + \boldsymbol{f} + \mu \nabla^2 \boldsymbol{u} + \sigma \kappa \delta_s \boldsymbol{n}, \tag{3}$$

where $\boldsymbol{u}$ is the flow velocity field, p is the pressure, ρ is the density, μ is the viscosity and $\boldsymbol{f}$ is the body force vector. The fourth term on the right hand side of Eq. (3) is a singular term, with a Dirac distribution function δ_s indicating the interface, and it represents the surface tension force. In the surface tension term, σ is the surface tension coefficient, κ is the local curvature and $\boldsymbol{n}$ is unit normal of interface. The position of each substance is defined by a color function C that takes the values of 1, 0 and a fractional number in the reference phase, second phase and interface cell, respectively. The interface position is then given by the solution of an advection equation for C

$$\frac{\partial C}{\partial t} + \boldsymbol{u} . \nabla C = 0 \tag{4}$$

The density and viscosity are correspondingly defined as

$$\rho = C\rho_l + (1 - C)\rho_g, \tag{5}$$

$$\mu = C\mu_l + (1 - C)\mu_g, \tag{6}$$

where the variables with subscripts "g" and "l" represent gas and liquid phases, in respect. The variables without a subscript indicate the local value based on VOF approach.

In this work, Basilisk solver is chosen to simulate atomization process. This solver applies VOF method to track the gas-liquid interface and estimate the material properties at the interface. The VOF method is implemented under the framework of octree adaptive mesh refinement. Also, The Navier–Stokes equations are solved by using CFL-limited time step, Bell-Colella-Glaz advection scheme and the implicit viscosity formulation. Projection approach is applied to decouple pressure and velocity in the Navier–Stokes equations. The conserving form of inertia term is implemented to avoid instability of the calculations due to the abrupt change of material properties at the interface.

The previous researches proved that breakup mechanisms is controlled by overall summation of viscous, inertia and surface tension forces at the interface. High gas viscosity can damp the instability leading to breakup of liquid jet. Consequently, the breakup point and jet topology change by increasing gas viscosity. In this paper, a parametric study is done on the atomization process in a wide range of gas-flow Reynolds numbers (Reg=39-39000) at low density ratio. The size, velocity and mass rate of droplets formed along jet column are studied and compared with experimental measurements.

A case with high weber number was chosen as the baseline. The flow chracteristics and fluid properties for the baseline case are mentioned in Table 1. We focus on the effect of gas Reynolds number and vary the dynamic viscosity of gas in four cases shown in Table 2. In this simulations, the coordinate system has the x-axis in the direction of liquid injection and the y-axis in the crossflow direction. The computational domain is a cube of $3.125cm \times 3.125cm \times 3.125cm$. The jet orifice is circular and the center of orifice is located at coordinate (0.0, 0.0, 0.0) with a diameter of $d0 = 0.8\ mm$. At $x = 0$ plane, no slip boundary condion is applied, except at the jet orifice where dirichlet boundary condition is imposed for jet inlet. At $y = -0.781cm$ plane, a dirichlet boundary condition is applied for inlet gas crossflow. Outflow boundary is implimented for the rest of boundary planes.Ten levels of grid refinement are used in all cases to refine the grid near the liquid-gas interface and capture the main small scales of turbulent flow in both phases. The finest grid size is set to be $\Delta x = 30.5\ \mu m$.

Table 1. Fluid properties and flow parameters for the baseline case (SI unit).

ρ_l	ρ_g	μ_l	μ_g	σ	d_0	U_l	U_g	r_ρ	q	We_g	Re_l	r_μ
997.0	59.0	8.94×10^{-4}	1.86×10^{-5}	0.0708	0.0008	35.4	15.5	16.9	88.5	160.2	31582.8	48.1

Table 2. Fluid properties for all the cases (SI unit).

Cases	ρ_l	ρ_g	r_ρ	μ_l	μ_g	Re_g	r_μ
1(baseline)	997.0	59.0	16.9	8.94×10^{-4}	1.86×10^{-5}	39000	48.1
2	997.0	59.0	16.9	8.94×10^{-4}	1.86×10^{-4}	3900	4.81
3	997.0	59.0	16.9	8.94×10^{-4}	1.86×10^{-3}	390	0.481
4	997.0	59.0	16.9	8.94×10^{-4}	1.86×10^{-2}	39	0.0841

Results and discussion

First, the plume boundary of the baseline case is validated. Then, a grid study is performed on the baseline case to explain how the grid size may affect the primary atomization and droplets size distribution. Finally, the characteristics of this case is compared with higher gas viscosity conditions. All the results discussed in this work are collected after reaching to quasi-steady condition. The trajectory for the spray plume is quantitatively post-processed from the simulation data and plotted in Figure 1. The trajectories are defined as the maximum and minimum x and z position of liquid surface for each y location. The boundary data are discretized using a y-increment of 0.835 mm. Too small increment size decreases the number of samples in each increment leading to a non-monotonic graph as it can be observed for the red graphs in Figure 1. The data were extracted by averaging over 55 snapshots in time for the baseline case. The upper boundaries (solid lines) in Figure 1.a represent the penetrations of the jets. The results show good consistency with previous study [24] for maximum boundary in jet penetration direction. However, a discrepancy is observed for minimum x boundary. Since Basilisk takes advantage of a high-order accurate VOF scheme and robust octree mesh adaptive, it can capture the surface breakups that are closer to the jet orifice. Therefore, the minimum x boundary of present study shows droplets that are closer to x axis. However, since the slope of both minimum x boundaries are approximately the same, the droplets in that zone experience the same drag/inertia ratio for both simulations. Consequently, these droplets have relatively equal penetration in x direction. In Figure 1.b, both cases show approximately the same penetration in depth direction as well.

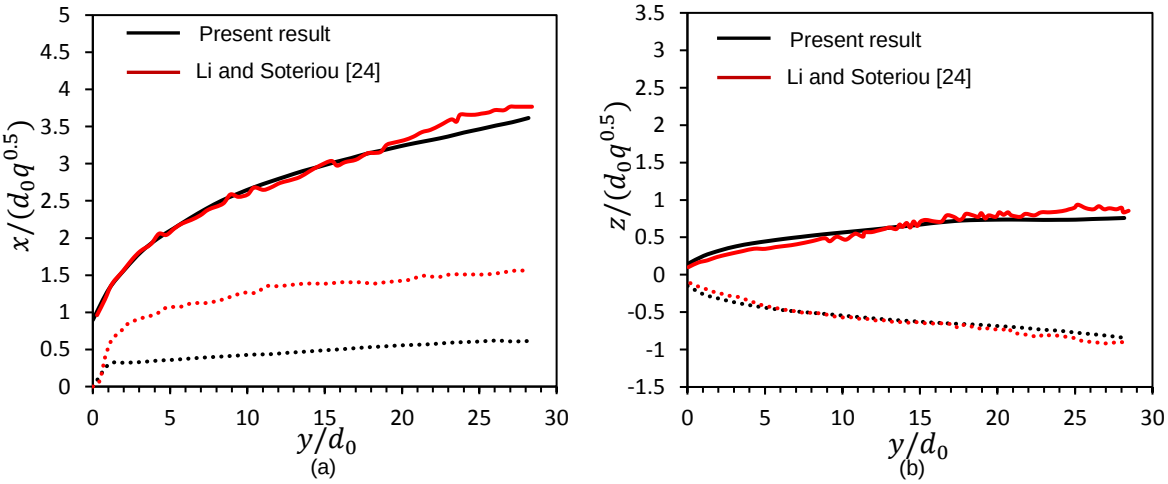

Figure 1. Comparison of spray plume boundary results in (a) jet inlet velocity direction (x) and, (b) depth penetration (z) for baseline case (Table 2) with Li and Soteriou [24]. Solid and dashed lines are used to represent the maximum and minimum boundary, respectively.

Figure 2 shows the atomization of baseline case for ten, nine and eight levels of grid refinement (Figure 2.b, 2.c and 2.d respectively). Also, it compares them with the study was done by Li and Soteriou [24] (Figure 2.a). As the grid size

reduces, the column breakup height and length decrease as well. Also, the onset of surface stripping happens closer to the jet orifice. All this changes are associated with the wavelength of instabilities formed on the jet column. Using a finer grid size better captures the small wavelengths responsible for jet breakup and surface breakup. When the wavelength of instabilities on the jet surface decreases, the size of droplets separated from jet column reduces. Therefore, the average droplet size for Figure 2.b is lower than 2.c and 2.d. The average wavelength was calculated for all the cases in Figure 2 and plotted in Figure 3. The trend of present results indicates a good consistency with the one was calculated in the literature [24].

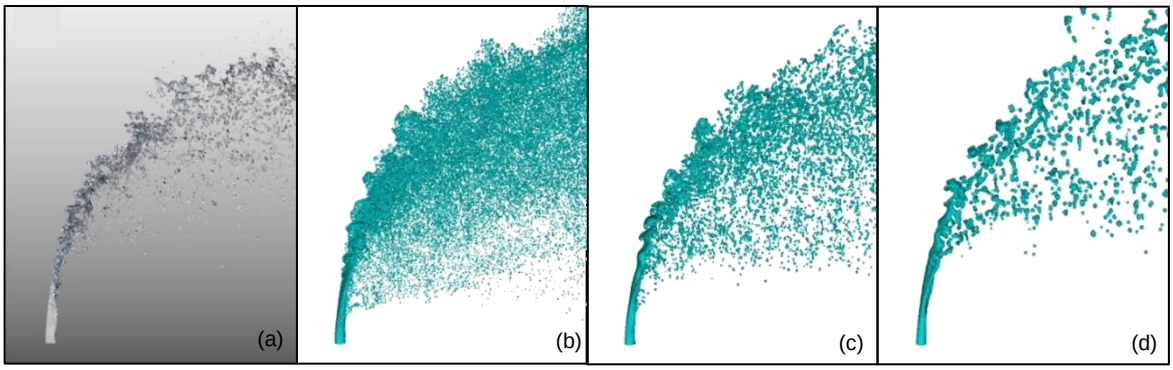

Figure 2. Comparing the results of baseline case for the different levels of grid refinement with the work of Li and Soteriou [24]: (a) Δx =39(μm) (Li and Soteriou [24]), (b) Δx =30.5(μm), (c) Δx =61(μm) and (d) Δx =122(μm).

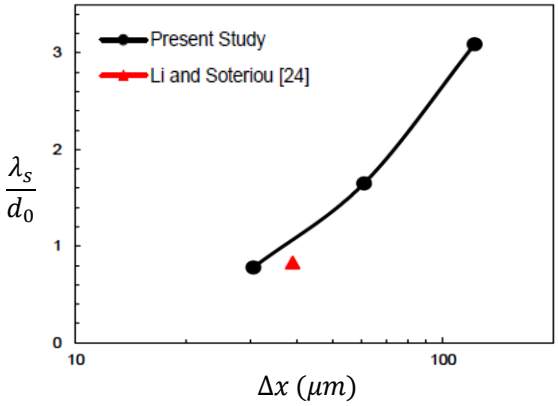

Figure 3. The effect of grid refinement on the wavelength of the instabilties formed on jet column is demonstrated for the baseline case. Tle black color and red color show the present study and Li and Soteriou results [24], respectively.

In Figure 4 and Figure 5, the atomization features of liquid jet in crossflow are qualitatively compared at different r_μ conditions. Figure 4 demonstrates the snapshots of liquid jet breakup in xy frame at $t = 0.0059s$. Also, Figure 5 shows the windward side of the jet at the same physical time. As the jets penetrate into the crossflows, they all bend towards the direction of the crossflow stream. Although the same momentum flux ratios are imposed for the all cases, the jets show different penetrations before column breakup (Figure 4), and this is associated with surface destabilization on the liquid column. As the viscosity of gas increases, the instability waves appear to be significantly damped out (Figure 5.c and 5.d). Consequently, the jet column penetrates more before breakup and a dramatic change in breakup point at the lowest viscosity ratio $r_\mu = 48.1 \times 10^{-3}$ (Figure 4.d) can confirm this behaviour. Also, the approximation of breakup length and height, mentioned in Table 3, show the same trend. As the destabilization waves become stronger (Figure 5.a and 5.b) the surface breakup starts closer to the jet orifice (Figure 4.a and 4.b).

Although the liquid weber numbers are the same for the all cases, the breakup mechanism, size and topology of separated ligaments vary for different viscosity ratio conditions. The near-field surface waves emerged on jet column change their characteristics. Also, the evolution of column shapes at different cross-section heights can confirm the change in the surface destabilization characteristics. As the height increases, the liquid column is more deformed,

developing transverse edges which are the primary sites for column stripping. As the gas viscosity decreases, the onset location for liquid stripping/breakup is shifted towards the injection orifice (Figure 4.a and 4.b). In addition, the size of separated droplets from jet surface are the smallest, when $r_\mu = 48.1$, and their shape are more close to sphere. On the other hand, in the case with the lowest viscosity ratio, the wavy perturbations are witnessed further from the location of jet orifice (Figure 5.d) and their wavelength is much larger than baseline case. Consequently, the liquid stripping is delayed. In addition, the reduced column stripping at lower gas Reynolds number flattens more the jet column. Since a larger cross-sectional area exposed to the crossflow, the drag force bends the jet column more toward the crossflow direction [16] (Figure 4.d).

In Figure 4.d, the growth of the mentioned surface waves causes the formation of ligaments that are further stretched from the transverse edges. These long ligaments appear as finger-shaped structures. The probability of breakup reduces for these long pinched-off ligaments. This phenomenon can be related to the effect of high viscosity of gaseous crossflow on damping the capillary waves on the ligaments.

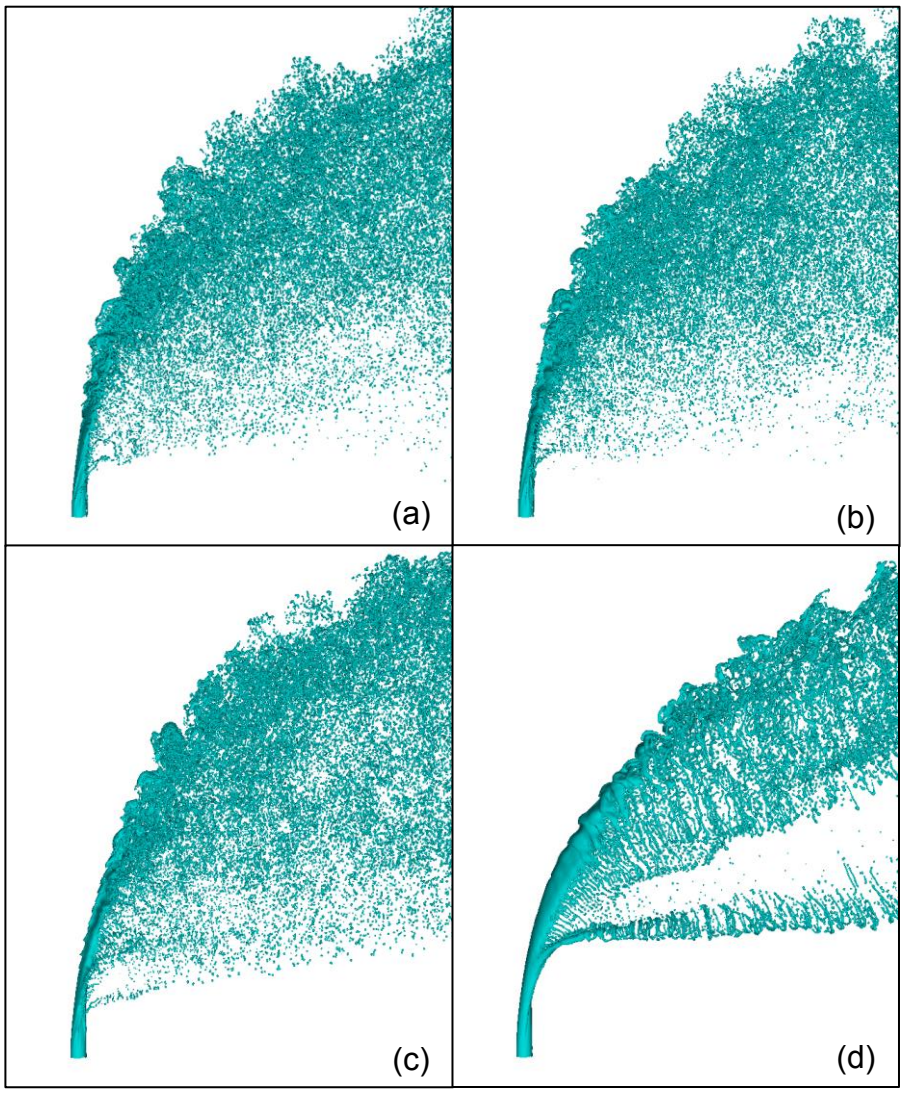

Figure 4. Instantaneous side view snapshots of liquid jet breakup in crossflow for different gaseous crossflow Reynolds number: (a) Re_g= 39000, (b) Re_g= 3900, (c) Re_g=390 and (d) Re_g=39.

In Figure 4, the ligaments that are formed due to the jet breakup have different features. As the gas viscosity increases, the ligaments formed are larger and they are more stretched out, especially in Figure 4.d. In the fourth case, although they have more area exposed to the crossflow, they do not intend to go under further breakups. So, a higher average

droplet size is expected for the fourth case. This phenomenon can be probably related to the effect of viscosity on reducing the intensity of turbulent flow in gas phase. Consequently, less instabilities are initiatetd on the legaments surface. On the other hand, in the case with the highest Reynolds number, the ligaments are smaller and their breakups continue until surface tension overcomes stroger inertia force. For this case, small droplets are formed and their shapes are much closer to sphere (Figure 4.a).

Table 3. Breakup locations at different viscosity ratios (SI unit)

r_μ	48.1	48.1×10^{-1}	48.1×10^{-2}	48.1×10^{-3}
$x_b/(d_0 q^{0.5})$	1.51	1.39	1.79	2.03
y_b/d_0	4.44	3.56	5.67	8.87

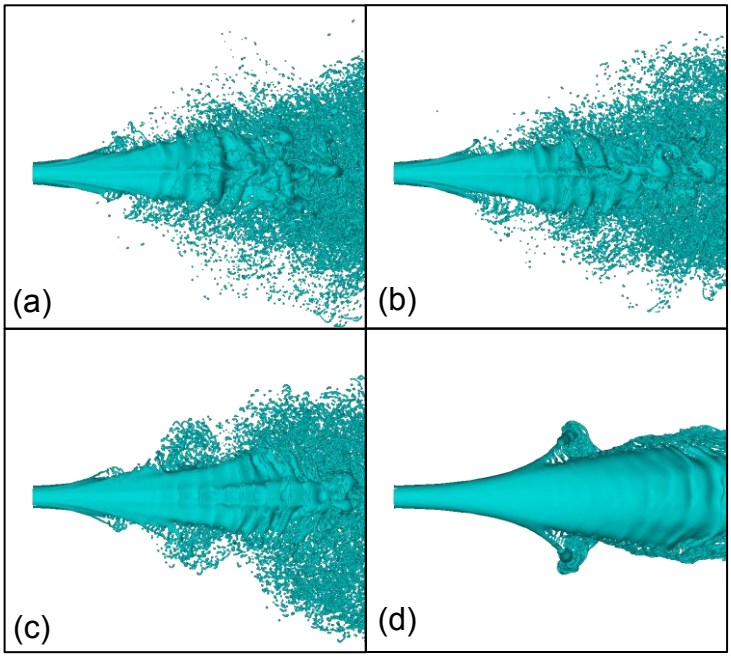

Figure 5. Instantaneous windward view snapshots of liquid jet breakup in crossflow for different gaseous crossflow Reynolds number: (a) Re_g= 39000, (b) Re_g= 3900, (c) Re_g=390 and (d) Re_g=39.

Conclusion

An investigation of the impact of gas viscosity variation on the liquid jet atomization in a gaseous crossflow has been performed using a validated simulation data. The effects of viscosity ratio were independently studied by maintaining the momentum flux ratio and Weber number at the fixed values for all cases. Higher viscosity of gas crossflow damps the instability waves appear on the jet surface. The results indicate that the breakup location is increased by increment of gas viscosity. Also, the separated ligaments have lower tendency for further breakup in high gaseous crossflows.

Nomenclature

$\boldsymbol{u}$ velocity vector [m s^{-1}]
ρ density [kg m^{-3}]
p pressure [N m^{-2}]
$\boldsymbol{f}$ force [N]
μ dynamic viscosity [kg m^{-1} s^{-1}]
σ surface tension coefficient [N m^{-1}]

y_b column breakup length [m]
x_b column breakup height [m]

References

[1] Sterling, A. M., and Sleicher, C. A., 1975, “The Instability of Capillary Jets,” J. Fluid Mech.

[2] McCarthy, M. J., and Molloy, N. A., 1974, “Review of Stability of Liquid Jets and the Influence of Nozzle Design,” Chem. Eng. J., **7**(1), pp. 1–20.

[3] Lefebvre, A. H., 1989, “Atomization and Sprays Hemisphere Publishing Corporation,” New York.

[4] Chigier, N., and Reitz, R. D., 1996, “Regimes of Jet Breakup and Breakup Mechanisms- Physical Aspects,” Recent Adv. spray Combust. Spray At. drop Burn. phenomena., **1**, pp. 109–135.

[5] Lin, S. P., and Reitz, R. D., 1998, “Drop and Spray Formation from a Liquid Jet,” Annu. Rev. Fluid Mech., **30**(1), pp. 85–105.

[6] Noh, W. F., and Woodward, P., 1976, “SLIC (Simple Line Interface Calculation),” *Proceedings of the Fifth International Conference on Numerical Methods in Fluid Dynamics June 28--July 2, 1976 Twente University, Enschede*, pp. 330–340.

[7] Hirt, C. W., and Nichols, B. D., 1981, “Volume of Fluid (VOF) Method for the Dynamics of Free Boundaries,” J. Comput. Phys., **39**(1), pp. 201–225.

[8] Youngs, D. L., 1982, “Time-Dependent Multi-Material Flow with Large Fluid Distortion,” Numer. methods fluid Dyn.

[9] Ahn, H. T., and Shashkov, M., 2007, “Multi-Material Interface Reconstruction on Generalized Polyhedral Meshes,” J. Comput. Phys., **226**(2), pp. 2096–2132.

[10] Osher, S., and Sethian, J. A., 1988, “Fronts Propagating with Curvature-Dependent Speed: Algorithms Based on Hamilton-Jacobi Formulations,” J. Comput. Phys., **79**(1), pp. 12–49.

[11] Sussman, M., Smereka, P., and Osher, S., 1994, “A Level Set Approach for Computing Solutions to Incompressible Two-Phase Flow,” J. Comput. Phys., **114**(1), pp. 146–159.

[12] Peskin, C. S., 1977, “Numerical Analysis of Blood Flow in the Heart,” J. Comput. Phys., **25**(3), pp. 220–252.

[13] Peskin, C. S., 2002, “The Immersed Boundary Method,” Acta Numer., **11**, pp. 479–517.

[14] Unverdi, S. O., and Tryggvason, G., 1992, “A Front-Tracking Method for Viscous, Incompressible, Multi-Fluid Flows,” J. Comput. Phys., **100**(1), pp. 25–37.

[15] Xiao, F., Wang, Z. G., Sun, M. B., Liang, J. H., and Liu, N., 2016, “Large Eddy Simulation of Liquid Jet Primary Breakup in Supersonic Air Crossflow,” Int. J. Multiph. Flow, **87**, pp. 229–240.

[16] Li, X., Gao, H., and Soteriou, M. C., 2017, “Investigation of the Impact of High Liquid Viscosity on Jet Atomization in Crossflow via High-Fidelity Simulations,” Phys. Fluids, **29**(8), p. 82103.

[17] Li, X., and Soteriou, M., 2013, “High-Fidelity Simulation of Fuel Atomization in a Realistic Swirling Flow Injector,” At. Sprays, **23**(11).

[18] Li, X., and Soteriou, M. C., 2016, “High Fidelity Simulation and Analysis of Liquid Jet Atomization in a Gaseous Crossflow at Intermediate Weber Numbers,” Phys. Fluids, **28**(8), p. 82101.

[19] Becker, J., and Hassa, C., 2002, “Breakup and Atomization of a Kerosene Jet in Crossflow at Elevated Pressure,” At. Sprays, **12**(1–3).

[20] Jabbari, F., Jadidi, M., Wuthrich, R., and Dolatabadi, A., 2014, “A Numerical Study of Suspension Injection in Plasma-Spraying Process,” J. Therm. Spray Technol., **23**(1–2), pp. 3–13.

[21] Mazallon, J., Dai, Z., and Faeth, G. M., 1999, “Primary Breakup of Nonturbulent Round Liquid Jets in Gas Crossflows,” At. Sprays, **9**(3).

[22] Lee, K., Aalburg, C., Diez, F. J., Faeth, G. M., and Sallam, K. A., 2007, “Primary Breakup of Turbulent Round Liquid Jets in Uniform Crossflows,” AIAA J., **45**(8), pp. 1907–1916.

[23] Popinet, S., “The Basilisk Code” [Online]. Available: http://basilisk.fr/.

[24] Li, X., and Soteriou, M. C., 2018, “Detailed Numerical Simulation of Liquid Jet Atomization in Crossflow of Increasing Density,” Int. J. Multiph. Flow, **104**, pp. 214–232.